NUMERICAL SIMULATIONS AND NON DESTRUCTIVE MEASUREMENTS OF FIBRE ORIENTATION ON UHPFRC WIND TOWERS

Fabrice Toussaint (1), Hervé Rouch (2) and Svatopluk Dobrusky (1)

(1) LafargeHolcim Research Center, France

(2) INOPRO, Villard de Lans, France

Abstract

The objective of this study was to test the capability of numerical tools to predict the orientation of fibres in various configurations of UHPFRC casting. A strong industrial challenge is to find the best casting configuration of very big windmill elements. Four different configurations were experimentally casted and tested in a reduced scale. Many samples were sawed in the tubes and their mechanical properties were characterized in both transverse and longitudinal directions. The orientation of fibres was measured on polished sections by optical methods, and also with a non-destructive magnetic device. Starting from rheological characterizations of the UHPFRC, and considering the exact geometry of the reduced scale elements which were poured, the free surface flow was simulated and the tensor orientation was fully described in some representative sampling locations. Conclusions are that the orientation trend is predicted by the numerical simulations and can be measured with the magnetic device.

Résumé

L'objectif de cette étude était de tester la capacité des outils numériques pour prédire l'orientation des fibres dans différentes configurations de coulage de BFUP. C'est en effet un défi industriel majeur de trouver la meilleure configuration de coulage de très gros éléments constitutifs d'éoliennes. Quatre configurations ont été coulées et testées à échelle réduite. De nombreuses éprouvettes ont été sciées au sein des tubes et leurs propriétés mécaniques ont été caractérisées dans les directions transverses et longitudinales. L'orientation des fibres a été mesurée par des méthodes optiques sur des sections polies, et aussi à l'aide d'un dispositif magnétique. A partir de caractérisations rhéologiques du BFUP, et considérant l'exacte géométrie des éléments à échelle réduite qui ont été coulés, l'écoulement à surface libre a été simulé et le tenseur d'orientation a été complètement décrit pour certains emplacements représentatifs de l'échantillonnage. Les conclusions sont que la tendance d'orientation est prédite par les simulations numériques et peut être mesurée par le dispositif magnétique.

1. INTRODUCTION

The main objective of this study was to assess the influence of the method of pouring a UHPFRC on the mechanical behaviour of a windmill structure. The pouring conditions have a strong impact on the fibre orientation [1]. Considering a given mechanical performance of the UHPFRC matrix, the first factor of influence is mainly the orientation of the fibres which has a strong influence on the tensile strength of the material [1], [2] and therefore on the flexural behaviour of the windmill tubes and the assembly mechanical parts.

As the real scale characterization of a windmill element is very hard to measure, it is of great interest to be able to predict the orientation of the fibres without pouring the elements. Ferrara *et al.* [3] demonstrated the capability of Computational Flow Dynamics to predict the fibre orientation in UHPFRC and to correlate with non-destructive measurements. The strategy which was implemented was to test the capability of prediction of the numerical simulation to predict the fibre orientation in different configurations of pouring. To achieve this objective, reduced scale elements were poured with the UHPFRC considered for this industrial project (Ductal®), with different configurations. We attempted to measure the fibres orientation with a non-destructive method and also with a more accurate optical method, on cut sections. All the results were compared to the mechanical performances measured on samples which were sawed in different positions of the tubes.

2. TECHNICAL APPROACH

Windmill tower geometry is complex when considered in detail. The system which is studied is a simplified and reduced scale of the real windmill geometry (Figure 1).

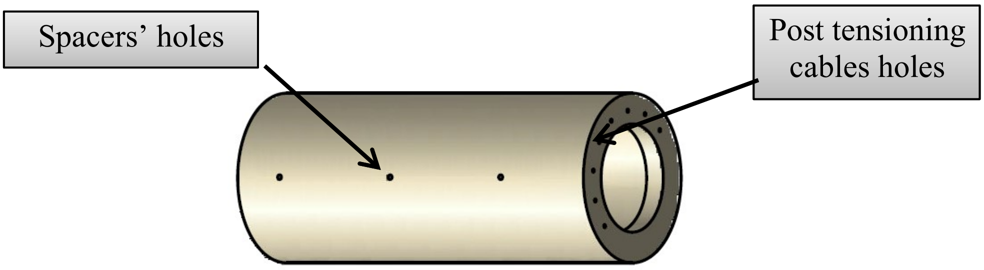

Figure 1 : description of the reduced scale tube with a flange

Table 1 : Pouring cases and related details

Case	Sketch	Case	Sketch
Case 2 : Gravity pouring fixed point	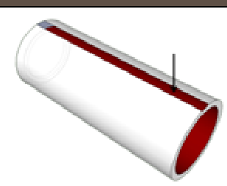	Case 1 : horizontal injection	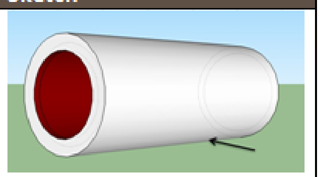
Case 3 : gravity pouring with a moving hopper	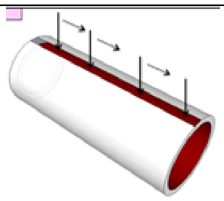	Case 4 : vertical injection	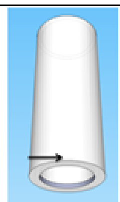

The reduced scale consists of tubes of 6 cm thickness, 1 m diameter and 2.5 m length while the real scale is slightly conical with a variable thickness from 6 cm to 15 cm, 4 m-diameter and 23 m length. A flange of 12 cm, which is dedicated to integrate the post-tensioning cables, is also a part of the reduced scale. On this reduced scale device, different ways of pouring the concrete have been tested. The horizontal and vertical pouring were considered and the injection method was compared with the gravity pouring method. The configurations of pouring are described in Table 1.

3. EXPERIMENTAL CHARACTERIZATION

3.1 Sampling for mechanical testing

Fifty-four samples were sawed from the different tubes in both longitudinal and transversal directions as described in Figure 2. The flexural strength and the limit of elasticity were characterized by a 4 point flexural test. The curvature of the samples doesn't seem to be critical regarding the representativeness of the measurement.

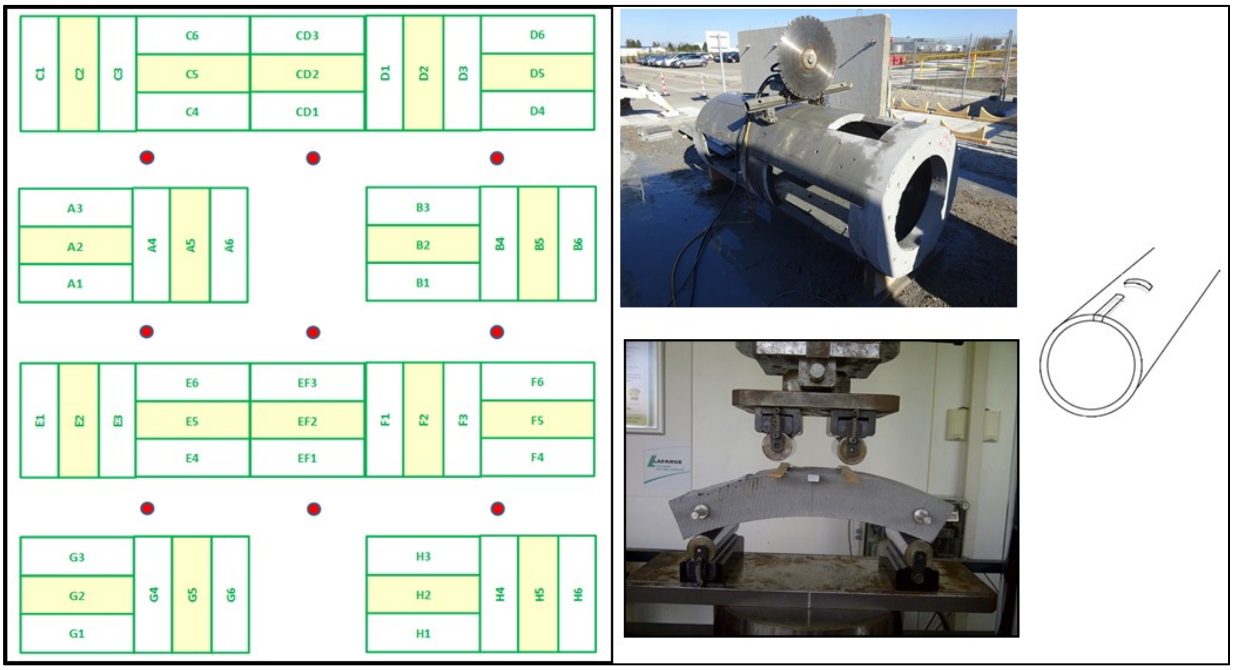

Figure 2 : Cutting plane of the samples in the tube

3.2 Magnetic measurements

A commercial pachometer, which was originally dedicated to detect rebars in the concrete was diverted to measure the orientation of the fibres. This device is actually sensitive to the metal and to a main orientation. It can be used as a non-destructive method to assess the main orientation of the fibres and the level of anisotropy as presented in Figure 3. By recording the value of the signal in a set of orientations by rotating in a 180° range, one can find the orientation and the level of the maximum signal and the minimum signal. We get therefore three outputs from the measurements which are the orientation θ_{Max}, the value of the max and min signals χ_{Max} and χ_{Min}.

The degree of anisotropy is given by $\xi = 2 \cdot \left(\frac{\chi_{max}-\chi_{min}}{\chi_{max}+\chi_{min}}\right)$

An index of "orientation quality" λ_o was computed from the experimental value. It has to be maximum when the angle θ_{Max} is in the longitudinal orientation of the sample in order to increase the flexural strength. It will be close to zero if ξ is close to zero (isotropy) or if θ_{Max} is near to 45° regarding the orientation of the sample. In the same way, it will be negative when approaching a transverse orientation compared to the sample.

λ_o ranges between -1.5 and +1.5.

The pachometer index λ_p is calculated as follows:

$$\lambda_p = \lambda_o \cdot (\chi_{Max} - \chi_{Min})$$

The index was proved as qualitatively representative of the orientation estimated by the way of optical measurements (Figure 4).

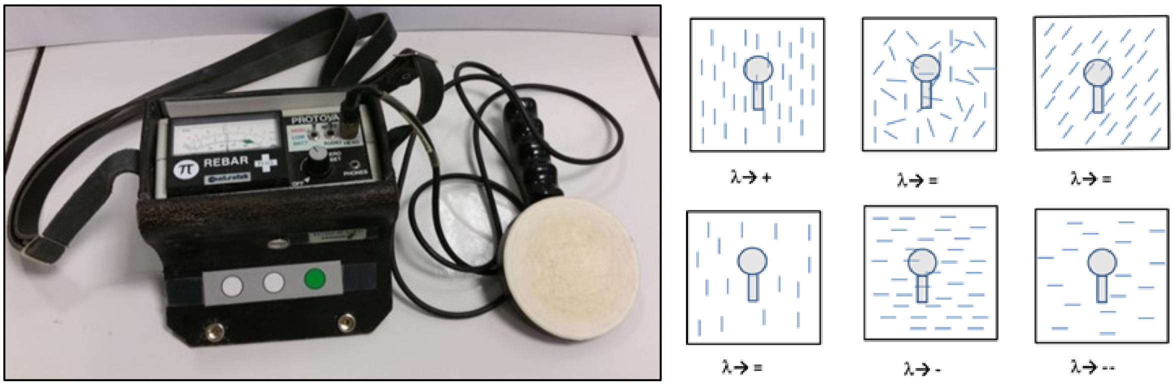

Figure 3 : Pachometer used to measure the orientation of fibres

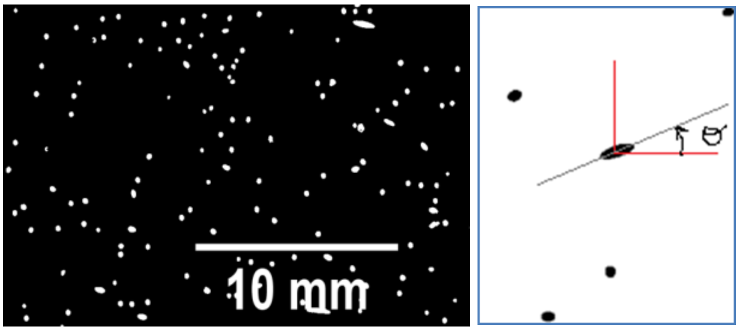

Figure 4 : Optical measurement of the orientation

3.3 Rheology of the UHPFRC

The rheology of Ductal® can be measured with a classical rheometer when it is considered without fibres. The measurement of the rheological behaviour with fibres is more tricky because of the size of the fibres (13 mm length and 0.2 mm in diameter) from one part and because the shearing tends to align the fibres from the other part.

A torque meter (Heidolph RZR 2102, see Fig. 5) with a self-designed tool, inspired from the original design of Tattersall was used for the rheological characterization with fibres. This geometry has been calibrated to give the shear stress and the shear rate from respectively the torque and the rotation velocity, with the method developed by P. Marchal and co-workers [4]. This geometry reduces a too much privileged orientation during the measurement.

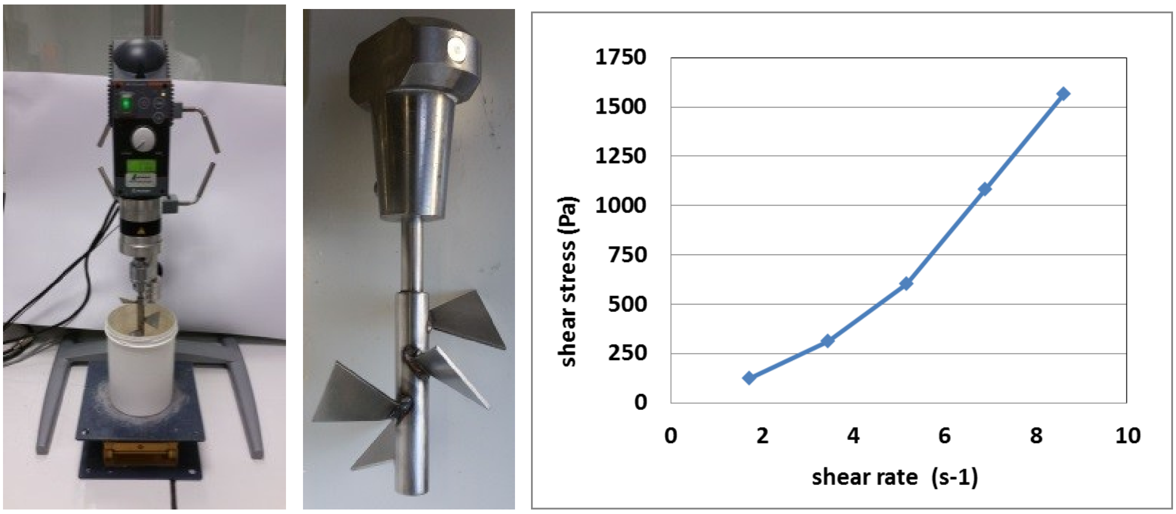

Figure 5 : Torquemeter and tool used for the UHPFRC characterization with fibres and typical rheogram

4. NUMERICAL SIMULATIONS

4.1 Methods and models

The presented results have been obtained using OpenFoam (www.openfoam.com). This choice has been done for several reasons:

- The code is "open", then all information about model, solver, and boundaries conditions are known and may be modified,
- As an alternative to other commercial CFD codes, it has faster solving due to other interface solving in the VOF model.
- It enables to use the different viscosity models,
- It enables to test a fiber orientation model.

The code was used to solve VOF (Volume Of Fluid) model with interface compression techniques (interface capturing methodology) [5]. The VOF model [6] is a two fluids model solving an average conservation equation. Following this type of two phase model, the transport models are similar for the two phases. Even if air is not under interest for this study, such two phases model are needed in order to model the Ductal® surface during casting.

Following these choices, the solved conservation equations are the following:

- Mass conservation of the mixed fluids:

$$\frac{\partial \rho}{\partial t} + \nabla \cdot (\rho U) = 0 \qquad (1)$$

where U is the velocity of the fluids and ρ the volume mass, ρ=2500kg/m³

- Momentum conservation:

$$\frac{\partial \rho \mathrm{U}}{\partial t} + \nabla \cdot (\rho \mathrm{U}\mathrm{U}) = -\nabla p^{*} + \nabla \cdot (\mu \nabla \mathrm{U}) + (\nabla \mathrm{U}) \cdot \nabla \mu - \mathbf{g} \cdot \mathbf{x} \nabla \rho + \sigma \kappa \nabla \gamma \quad (2)$$

where μ is the fluids viscosity, σ is the surface tension at the interface between the two phases, κ is the interface curvature, and γ is the indicator function which is the gas volume fraction. For immiscible fluids modelled by VOF methodology, it is equal to 0 in the liquid phase and to 1 in the gas phase, and between 0 and 1 if the interface cross the mesh volume.

In this study the viscosity of the liquid is derived from the Casson model:

$$\sqrt{\tau} = \sqrt{\tau_c} + \sqrt{\beta . \dot{\gamma}} \quad (3)$$

where τ is the shear stress, γ the shear rate, and with the following values : τ_c=22 Pa, β=45.

All these conservation equations are similar to the one solved for one phase flow. For two phases flow solved by VOF methodology the indicator function is solved, using a compression technique of the interface:

$$\frac{\partial \gamma}{\partial t} + \nabla \cdot (\mathrm{U}\gamma) + \nabla \cdot (\mathrm{U}_r \gamma (1-\gamma)) = 0 \quad (4)$$

where Ur is the compression velocity.

The transient solution procedure is very common, and is referred as PISO [7].

The fiber orientation model is derived from Jefferys model [8], neglecting fiber inertia and assuming an infinitely large liquid space and no fiber-fiber interactions:

$$\frac{\partial q}{\partial t} = W.q + \lambda F . (D.q - q.(q.D.q)) \quad (5)$$

where q is the fiber orientation vector, D the rate of strain tensor, W the vorticity tensor, and λF is a dimensionless fiber shape factor. A spherical particle has λF = 0, whereas very long fibres have λF → 1.

Using the orientation tensor of 4th order A, this model is written by Advani [9]:

$$\frac{\partial A}{\partial t} + (U.\nabla)A = -(\mathrm{W.A} - \mathrm{A} \cdot \mathrm{W}) + \lambda F (D.A + A.D - 2D{:}A(4)) + 2Dr(\delta - 3A) \quad (6)$$

where Dr is the rotary diffusion coefficient of the fibres.

A closure approximation is necessary for the calculation of the tensor of fiber orientation from the 4th order tensor A(4) obtained from Advani model solving. The closure approximation from Chung [10] is used.

The numerical results of the orientation are represented by the orientation tensor A $\left\{\begin{matrix} a_{11} & a_{12} & a_{13} \\ a_{21} & a_{22} & a_{23} \\ a_{31} & a_{32} & a_{33} \end{matrix}\right\}$ where each column vector is one vector of the ellipsoid of orientation. In case of perfect orientation, only one vector has a magnitude equal to 1. On the contrary, in case of no orientation, the diagonal values of the tensor are equal to 1/3.

Some classical boundaries conditions are used for all these models: a reference pressure is fixed to 0 (relative pressure) where air is coming out; liquid flow rate is assumed on injection points; no fiber orientation on the injection points (an orientation due to the velocity appear in the flow)

4.2 Results of numerical simulation

Three different configurations, represented in Figure 6, among the four tested experimentally were tested by the numerical simulation method. These configurations are the numbers 1, 2 and 4 from Table 1.

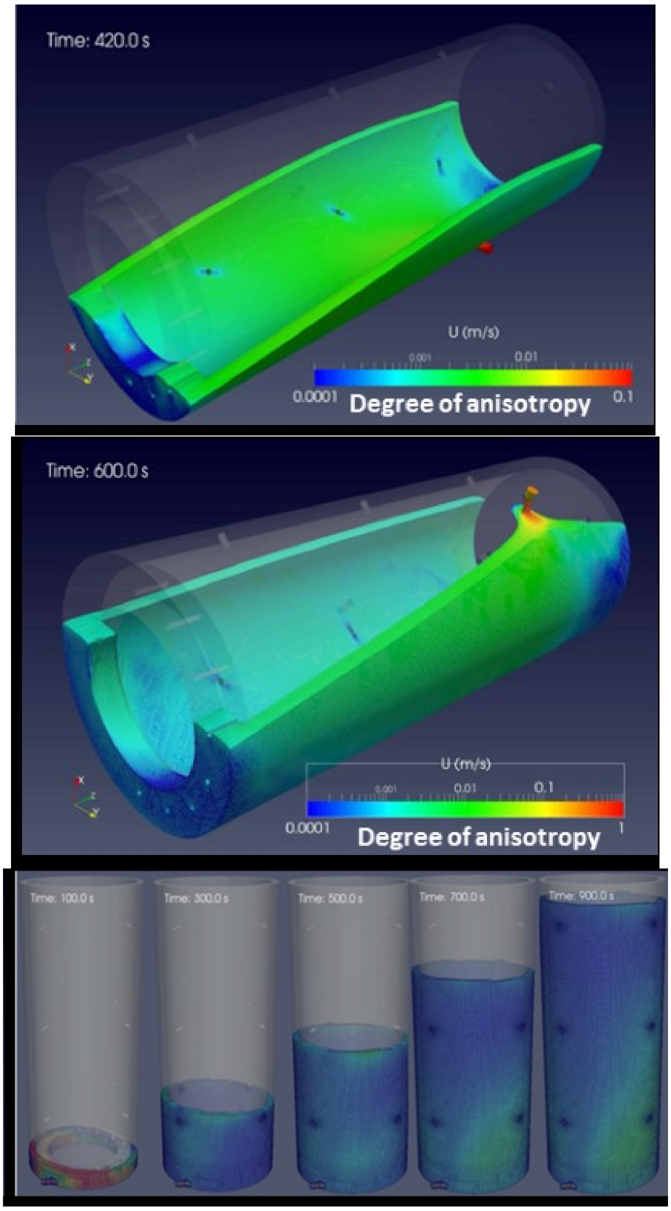

Figure 6 : screenshots of the simulation in the 3 configurations (1, 2, 4) from top to bottom

Some critical points in the geometry were chosen as they are representative of the experimental samples which were sawed, and characterized by flexion and with the pachometer. The numerical results of the tensor were extracted for the configuration 1 and 4, selected arbitrarily in 5 different points for each geometry. The longitudinal component of the tensor (i.e. in the direction of the tube) has been extracted from the results. The orientation is assumed to be never perpendicular to the layer thickness. It was moreover verified by the image analysis. Considering this hypothesis, a very basic index representative of the quality of the orientation for a given sample has been built: for samples which are longitudinal: $\kappa = a_{33}$; for samples which are transverse: $\kappa = 1 - a_{33}$

A higher value of κ is representative of a stronger orientation of the fibres in the direction of the samples, whether they are in the transverse or longitudinal direction of the tube.

5. COMPARISON OF RESULTS

The main objective of the study was to assess the capability of prediction and the limit of the numerical simulation to predict the orientation of fibres in relatively complex pouring situations and geometries. It is also of interest to study the non-destructive methods like the magnetic method which is proposed. Therefore we compare in Figure 7 the flexural strength (averaged on 3 samples) and the index λ_p which was computed from the pachometer measurements. The correlations are far from perfect but they are nevertheless significant, regarding the capability of the pachometer to detect the fibres orientation.

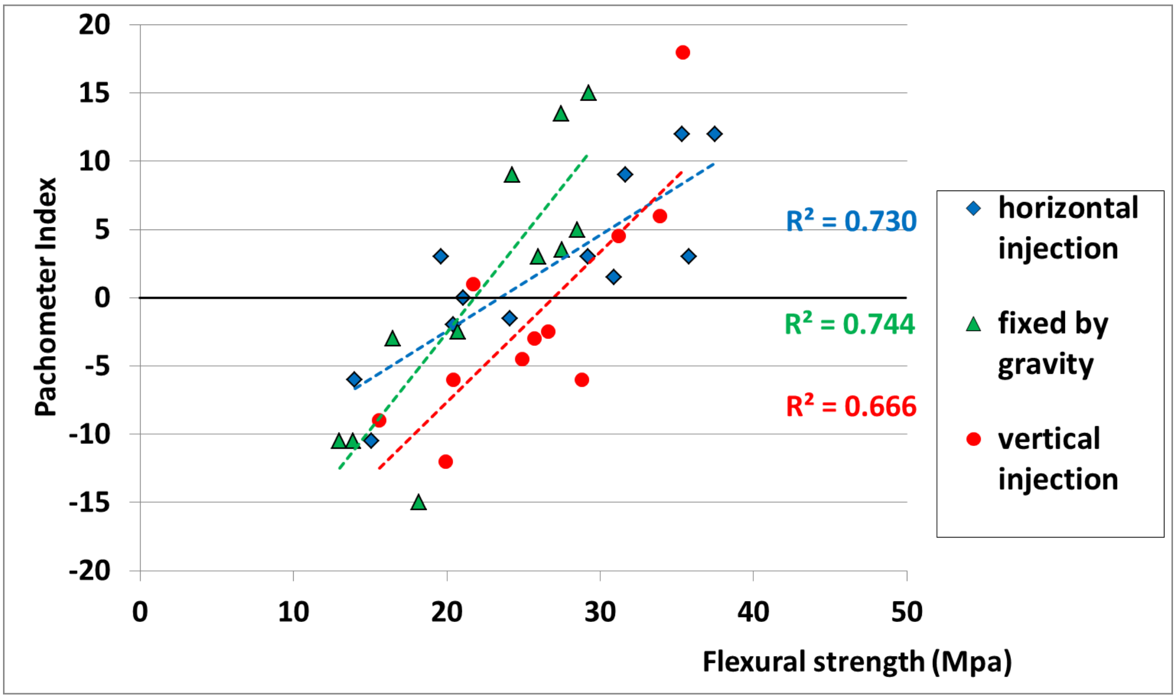

Figure 7 : Correlation between the flexural strength and the pachometer index for different pouring configurations

κ is supposed to be correlated with the flexural strength, as the orientation of the fibres is the key parameter regarding this mechanical property. The correlations between ***κ*** and the flexural strength of the corresponding samples are plotted in Figure 7. A very good correlation is observed in the case of the horizontal injection and a relatively poor correlation in the vertical injection configuration. The global trend is nevertheless positive as one must keep in mind some artifacts as the curvature of the sample when characterized in transverse situation and a relatively poor repeatability with only 3 flexural measurements. The average standard deviation on the flexural measurements is close to 5 MPa, which can explain a part of the discrepancy in the correlations of Figure 8.

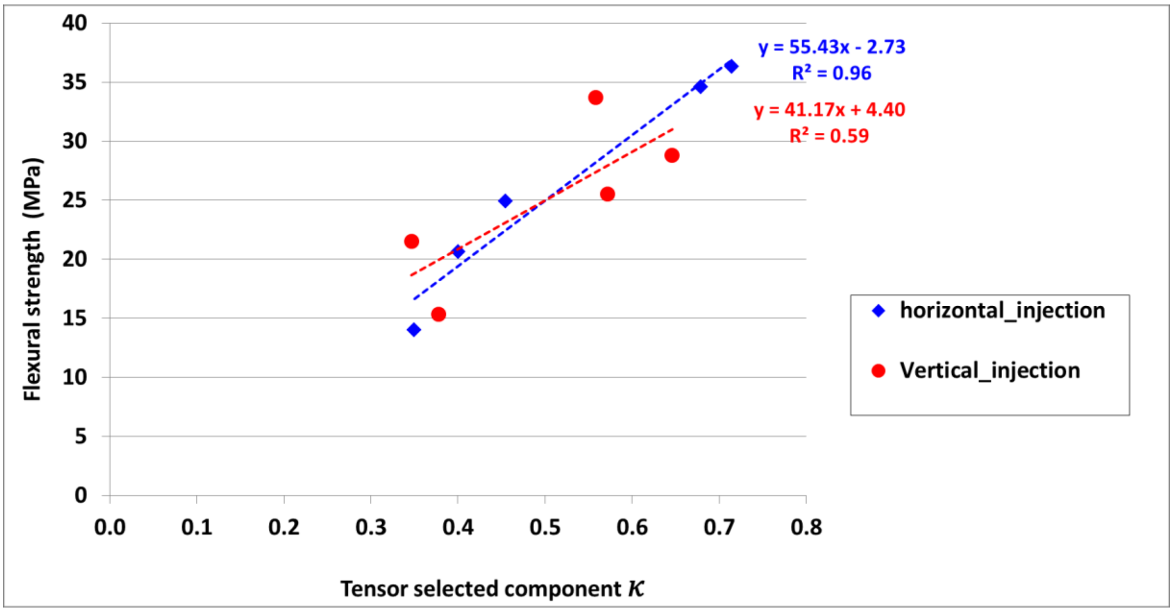

Figure 8 : correlation between numerical results in selected locations and their equivalent compressive strength in the horizontal and vertical injection configurations

6. CONCLUSIONS

The numerical simulations of different methods of casting reduced scale elements of a windmill were a quite successful. A good agreement was found between the flexural strength of the samples which were sawed in different locations in the tubes and their corresponding indexes issued from the numerical simulations.

A non-destructive magnetic method was also developed by using a rebar detector with a specific use. The correlations between the orientation found by this device and the corresponding flexural strength is also rather good.

The possibility of using the numerical simulation in complex geometries was validated which opens good industrial perspectives regarding the optimization of the casting process and the design of elements.

REFERENCES

[1] Baril, M.A., Sorelli, L., Rethore, J., Baby, F., Toutlemonde, F., Ferrara, L., Bernardi, S., Fafard, M.: "Effect of Casting Flow Defects on the Crack Propagation in UHPFRC Thin Slabs by Means of Stereovision Digital Image Correlation", Construction and Building Materials, 129, December 2016, pp. 182-192.

[2] Kang, S.-T. and J.-K. Kim, The relation between fiber orientation and tensile behavior in an Ultra High Performance Fiber Reinforced Cementitious Composites (UHPFRCC). Cement and Concrete Research, 2011. 41(10): p. 1001-1014.

[3] Ferrara, L., Cremonesi, M., Faifer, M., Toscani, S., Sorelli, L., Baril, M.A., Réthoré, J., Baby, F., Toutlemonde, F. and Bernardi, S.:"Structural elements made with highly flowable UHPFRC: correlating Computational Fluid Dynamics (CFD) predictions and non- destructive survey of fiber dispersion with failure modes", Engineering Structures, 133, February 2017, pp. 151-171

[4] Aït-Kadi, A., Marchal, P., Choplin, L., Chrissemant A.S., Bousmina, A.S., Quantitative analysis of mixer-type rheometers using Couette analogy, Can. J. Chem. Eng., 80, 1166-1174 (2002).

[5] Rusche Henrik, 2002, "Computational fluid dynamics of dispersed two-phase flows at high phase fractions", Ph-D thesis, Imperial College of Science, Technology & Medecine, London RU.

[6] Hirt C. W. and Nicols. B. D. 1981 "Volume of fluid (VOF) method for the dynamics of free boundaries". J. Comp. Phys., 39:201-225.

[7] Issa R. I., 1986, "Solution of the implicitly discretised fluid flow equations by operator splitting." J. Comp. Phys., 62(1):40 65.

[8] Jeffery, G., The motion of ellipsoidal particles immersed in a viscous fluid, Proc. Roy. Soc. London A 102 (1922), 161.

[9] Advani, S. G. und Tucker III, C. L., The Use of Tensors to Describe and Predict fiber Orientation in Short Fiber Composites, Journal of Rheology 31 (1987), Nr. 8, 751–784.

[10] Chung, D. und Kwon, T., Invariant-based optimal fitting closure approximation for the numerical prediction of flow-induced fiber orientation, Journal of Rheology 46 (2002), Nr. 1, 169–194.